The Structure and Tensile Behavior of First Year Sea Ice and Laboratory-Grown Saline Ice

by

G.A. Kuehn, R.W. Lee, W.A. Nixon and E.M. Schulson

Thayer School of Engineering
Dartmouth College
Hanover, New Hampshire 03755

September 1987

(Submitted to Proceedings OMAE '88)

Report No. IRL87/88 - 029

The Structure and Tensile Behavior of First Year Sea Ice and Laboratory-Grown Saline Ice

G. A. Kuehn, R. W. Lee, W. A. Nixon and E. M. Schulson

Thayer School of Engineering
Dartmouth College
Hanover, NH 03755

Abstract

Tensile tests have been performed on first year sea ice and on laboratory-grown saline ice at -10° C and at two strain rates, 10^{-3} s^{-1} and 10^{-7} s^{-1}. The first year sea ice was collected from the Beaufort Sea in April of 1983 and November of 1984. The laboratory-grown saline ice was grown unidirectionally downward by means of a cooling plate on an insulated tank. The ice was loaded both parallel (vertical orientation) and perpendicular (horizontal orientation) to its growth direction. The results showed brittle behavior at the higher rate for both orientations, but ductile behavior at the lower rate for the horizontally loaded ice. At both strain rates, both the tangent modulus and the tensile strength are significantly higher along the vertical direction. The structure and mechanical properties of the laboratory-grown ice were similar to those of the first year sea ice, indicating that the laboratory ice is a convenient and economical material for studying the mechanical properties of columnar saline ice.

Introduction

With the objective of exploring the tensile properties of saline ice, this paper presents: (a) a procedure for producing laboratory-grown saline ice (LGS ice), (b) a comparison between the structure of LGS ice and first year sea ice, (c) a technique for controlled high strain rate ($\dot{\varepsilon} = 10^{-3}s^{-1}$) uniaxial tension testing, (d) and some first results from uniaxial tension tests at -10 °C, at $\dot{\varepsilon} = 10^{-3}s^{-1}$ and $10^{-7}s^{-1}$, on vertically oriented LGS ice and first year sea ice and on horizontally oriented LGS ice. The procedure allows a convenient and economical method for obtaining test material, and the results compare favorably with those obtained previously by Dykins (1970).

Experimental Procedure and Ice Structure

A. LGS Ice

The ice was grown in a 250 gallon nalgene tank 36 inches in diameter and 48 inches deep. The tank was filled with tap water and "Instant Ocean" (a commercial product which contains all the salts contained in sea water in the proper proportions) to a bulk salinity of 20 ppt. On the top of the tank a freezing plate was placed to effect unidirectional (downward) freezing and thus to simulate a natural condition. The plate was fabricated from aluminum and plexiglass and contained a cavity through which ethylene glycol was pumped following refrigeration in a cooling bath. The growth was effected in a cold room set at 0° C. Once the solution and the cold plate had equilibrated, the sides of the tank were insulated, the bath temperature was reduce to -32.5° C (the lowest available), and a pressure relief valve at the bottom of the tank was opened. The ice was removed with a hoist when it reached a thickness of 12 to 14 inches, which usually took two to three weeks. From each block 15 to 22 specimens, 4 inches in diameter, were obtained by coring and then stored at -10° C. Figure 1 illustrates the insulated tank and the removal of a block of ice.

The growth rate of the ice can be controlled by the temperature of the coolant which circulates through the freezing plate. To increase the cooling capacity of the cold plate, the coolant was refrigerated using two baths in some cases. Figure 2 illustrates typical plots of the ice thickness and the bath temperature against time for one cooling bath (Block 5) and for two cooling baths (Block 6). The curves show that the temperature of the bath reached a plateau when the ice thickness was approximately 6 inches. The plateau temperature for Block 6 was considerably lower than for Block 5, which is consistent with Block 6 having twice the cooling capacity. To a first approximation, the growth rate was initially constant, owing to the increasing temperature difference between the cold plate and the salt water.

The ice was characterized by measurements of melt-water salinity, density, brine-pocket platelet spacing, grain size, grain shape and c-axes orientations. The melt-water salinity was determined using a temperature-compensated conductivity meter. The density was determined by comparing the weight of the ice in air to that in iso-octane at - 10° C. Thin sections were used to examine the grain size and shape, and the platelet spacing. The c-axes orientations were determined from thin sections which were examined using a Rigsby stage. The grain size was described by the average equivalent column diameter and by the average column length. The equivalent diameter was computed from the

average grain area within the cross section of a core. The column length was measured directly from vertically oriented thin sections taken from vertically oriented cores. Typical results are presented in Table 1. A salinity of 4 ppt at -10° C corresponds to a brine volume of about 2.2% (Cox and Weeks, 1983).

Thin sections typical of LGS ice are shown in Figure 3. From the top to the bottom of a core, the equivalent column diameter increases by a factor of about three. To within the accuracy of measurement (± 3°) the c-axes were randomly oriented within the plane of the block (i.e., perpendicular to the growth direction). The higher growth rate achieved with the two cooling baths increased the salinity by approximately a factor of 2, but did not noticably change the grain size or shape, the platelet spacing or the c-axes orientations, Table 1.

To determine whether the structure of the ice varied with location within the parent block, an examination was made of thin sections from cores taken systematically across the diameter of two blocks. One block was frozen with one cooling bath and the other with two. In all cores the structure was essentially the same as that described above and noted in Table 1. The structure of the ice thus appears to be independent of its location within the block.

B. Sea Ice

First year sea ice from the Alaskan Beaufort Sea was provided by Exxon Production Research (EPR) Company. The ice was harvested near the Prudhoe Bay West Dock Causeway in April 1983 when approximately 72 inches thick and in November 1984 when about 19 inches thick. It was stored at temperatures below -26° C in the EPR Houston facilities until February 1987 when it was shipped to Dartmouth where it was stored at -10° C.

There were no significant differences between the first year sea ice harvested in November of 1984 and that harvested in April 1983. Table 1 contains the first year sea ice structural information for comparison to the LGS ice structure, and Figure 4 illustrates the microstructure. The salinity, grain size and platelet spacing of LGS ice and that of the first year saline ice are very similar, suggesting that the LGS ice is a good structural analogue of first year sea ice.

Table 1.

Structure Comparison: **LGS Ice:** Block 3 (one cooling bath) and Block 6 (two cooling baths)
First Year Sea Ice: Harvested in Nov.1984 and Apr.1983 from the Alaskan Beaufort Sea

	Material		
Property	LGS Ice 1 cooling bath	LGS Ice 2 cooling baths	Sea Ice
Salinity (ppt)	4.3 ± 0.2	7.2 ± 1.0	
Nov. 1984			4.3 ± 0.3
Apr. 1983			4.2 ± 0.4
Density (kg/m^3)	914 ± 3	916 ± 2	
Platelet Spacing (mm)	0.5 - 1.0	0.5 - 1.0	0.5 - 1.0
Column Length (cm)	5 - 17	5 -18	
Grain Size* (mm) top	1.6 ± 0.3	2.2 ± 0.4	
mid	3.9 ± 0.6	3.7 ± 0.5	4.2 ± 0.6
bottom	5.2 ± 0.5	6.5 ± 0.6	

* grain size was calculated as the equivalent diameter, described in text.

C. Tensile Sample Preparation

In order to apply a uniaxial tensile load, phenolic resin (Synthane) end-caps with jute-backed carpeting epoxied to one surface were bonded to each end of the ice sample. The carpeting increases the strength of the end-cap/ice interface and dissipates the shear stresses which develop at the interface during testing.

To obtain good alignment of the end-caps the core was clamped in a milling machine and the ends were milled perpendicular to the long axis. Using the same clamp, the core was transferred to an alignment jig which maintained the position of the end-cap and the core during bonding. A latex membrane insured that the carpet remained saturated with water during freezing and accommodated the freezing strain. At the time of capping, the top and the bottom of vertically oriented cores (relative to the parent block) were recorded. Similar procedures for mounting end-caps for uniaxial tension testing have been described by Lee (1986) and by Cole *et al.* (1985).

To avoid excessive brine drainage, the vertical cores were stored in a horizontal position and the horizontal cores were stored in a vertical position. The overall storage time at -10° C (i.e., block removed to testing) varied from about 2 weeks to 27 weeks, with no apparent systematic effect on the propertiess measured.

Right circular cylinders (4 in. in diameter x 10 to 12 in.) were tested except for vertical specimens rapidly ($\dot{\varepsilon} = 10^{-3}s^{-1}$) strained (see below).

D. Testing Procedure

LGS ice was tested under uniaxial tension at a high ($10^{-3}s^{-1}$) and at a low ($10^{-7}s^{-1}$) strain rate with orientations both parallel (vertical orientation) and perpendicular (horizontal orientation) to the growth direction. The Alaskan Beaufort Sea Ice was only of vertical orientation. It was tested at the same strain rates as the LGS ice. All tests were performed in a cold room at -10° C ± 0.2° C on a closed-loop servo hydraulic materials testing machine. Test results were recorded on graphs of stress versus strain with an X-Y plotter.

Fracture generally occured within the gauge section of the specimens. However, when vertically oriented cores were tested at $10^{-3}s^{-1}$ as right circular cylinders, the ice/carpet interface invariably debonded. To avoid this problem, the cores were reduced in diameter by turning on a lathe to diameters between 2.920 to 3.154 inches. Strain gauge extenders were made to define a 5.5 inch gauge length. Using pads frozen to the ice (to reduce the stress concentration produced by the "knife edge" of the extensometers) and rubber bands, two strain gauges were attached directly to the necked section of the sample, see Figure 5. This practice provided direct strain measurement on the ice and a much simpler procedure mathematically than others previously used, described by Mellor *et al.* (1984). The output of the pair was averaged and the average was used to control the velocity of the actuator of the test machine to maintain a constant strain rate. Fractures in all cases occured within the reduced section and away from the fillets.

The strain gauge instrumentation of all low rate and high rate horizontally oriented tests was originally mounted to collars attached to the end-caps. This procedure was later discontinued in favor of mounting the extensometers directly to the samples, in the same manner as used with the necked

samples. During all tests, the strain rate was held constant.

Test Results and Discussion

Figure 6 shows stress-strain curves typical of the LGS ice and of the first year sea ice. At the higher strain rate, both the horizontally and the vertically oriented samples produced nearly linear curves which terminated in fracture after very little strain ($< 2 \times 10^{-4}$). At the lower strain rate, the curves for vertically oriented samples had negative curvature and terminated at approximately two times the strain of vertically oriented samples tested at the higher rate. At the lower strain rate, the curves for material of horizontal orientations displayed a peak. Subsequently, the stress fell slowly and then ended in fracture. While brittle tensile behavior is well known, the ductile behavior of the lower rate horizontal specimens is somewhat unusual. Possibly, as under low rate compression, the peak may denote a restorative process such as dynamic recrystalization.

The tensile properties vary with the sample orientation and to a lesser extent with the strain rate, Table 2.

The initial tangent modulus shows that the vertically oriented cores are stiffer than the horizontally oriented cores tested under the same conditions. For each orientation, the ice had a larger initial tangent modulus at the higher strain rate.

The tensile strength of the vertically oriented specimens is three to four times that of the horizontal samples, more or less in agreement with Dykins (1970). Specifically, at $10^{-7}s^{-1}$ the average strength of the vertical specimens was 1.02 ± 0.12 MPa compared with 0.28 ± 0.06 MPa for the horizontal specimens. At $10^{-3}s^{-1}$, the average strengths of the vertical and horizontal specimens respectively, was 1.25 ± 0.22 MPa and 0.35 ± 0.15 MPa. The tensile strength increases with strain rate for each orientation, but the effect is a small one relative to the orientation effect, Figure 7. The first year sea ice shows more variation than the laboratory ice and greater scatter was observed at the higher strain rate. Yet the LGS ice results are well within the range of the first year sea ice at both strain rates, showing that the LGS material is not only a structural but also a mechanical analogue of sea ice.

The strain rate has a greater effect than the orientation on the fracture strain. At the higher rate for both vertical and horizontal orientations, fracture occured at low strains ($< 2 \times 10^{-4}$). Since fracture of the horizontal high rate test specimens occurs at significantly lower stresses, they do not experience as much strain as the vertical samples. At the lower rate, the horizontal specimens reached axial strains of 2.8×10^{-3} to 8.8×10^{-3} at fracture, indicative of significant plastic deformation. This may arise from the horizontal samples being oriented so that basal planes (the easy slip planes) are well aligned for slip, while in the vertical samples the basal planes are essentially parallel to the loading direction.

Specimens vertically oriented and strained at $10^{-7}s^{-1}$ failed along a plane perpendicular to the loading direction. All of these samples failed where the column diameter was the largest, regardless of the orientation of the sample in the testing machine, Figure 8. This point suggests that the tensile strength of saline ice, like that for fresh-water ice, decreases with increasing grain size. Specimens vertically oriented and strained at $10^{-3}s^{-1}$ also failed along a plane perpendicular to the loading

direction and in this case, the fracture surface revealed transgranular cleavage facets, Figure 9. Specimens oriented horizontally and strained at $10^{-7}s^{-1}$ exhibited shear failures parallel to the growth direction (the columns axes), Figure 10, while the horizontally oriented samples strained at $10^{-3}s^{-1}$ failed along a plane perpendicular to the loading direction, Figure 11. These failure characteristics are summarized in Table 3. Again, no distinction could be made between the laboratory grown and the field ice.

It is interesting to note that in general terms the tensile behavior of columnar saline ice is similar to that of fresh-water ice, a least at -10° C. Both kinds of material exhibit a pronounced dependence of strength on the orientation of the loading direction. Both display only a small dependence of strength on the strain rate in the range explored here. And, both kinds of ice exhibit a brittle to ductile transition upon decreasing the strain rate from $10^{-3}s^{-1}$ to $10^{-7}s^{-1}$ (see Lee and Schulson 1987 for fresh-water behavior). These similarities reflect the fact that saline ice, although a multi-phase material (pure ice + brine + air + precipitated salts?), is composed predominantly of pure ice. The principal differences are that saline ice is weaker and more compliant, owing mainly to the presence and to the distribution of the pockets of brine.

Concerning the strength limiting mechanisms operative within saline ice, it could be argued that crack nucleation limits the high-rate strength while crack propagation limits the low-rate strength. Supporting this view is the shape of the stress-strain curves. At the higher rate the linearity suggests that, as in fresh water ice strained at the same rate and temperature (Lee and Schulson 1987), fracture corresponds to the nucleation of the first crack to form; i.e., to the immediate propagation of the first crack once it nucleates. At the lower rate, the negative curvature suggests that, again as in fresh-water ice (Lee and Schulson 1987), fracture occurs when the tensile stress is sufficiently high to propagate cracks which nucleated at lower stress (and strain). It must be cautioned, however, that such an arguement is not conclusive. The linear behavior, for instance, could depict the propagation of pre-existing defects, such as crack-like arrays of brine pockets, and not the stress to nucleate fresh cracks. Before conclusions can be drawn, detailed studies are needed on the effect of the scale of the microstructure on the tensile strength.

Conclusions

1. A procedure has been established for growing in the laboratory columnar saline ice which mirrors the structure and the tensile behavior of first year sea ice.

2. Tensile tests at a controlled strain rate of $10^{-3}s^{-1}$ on vertically oriented saline ice were performed by necking the samples and by mounting strain instrumentation directly to the necked region.

3. The tensile strength at -10° C increases slightly with an increase in strain rate, from 1.02 ± 0.12 MPa at $10^{-7}s^{-1}$ to 1.25 ± 0.22 MPa at $10^{-3}s^{-1}$ for vertically oriented samples and from 0.28 ± 0.06 MPa at $10^{-7}s^{-1}$ to 0.35 ± 0.15 MPa at $10^{-3}s^{-1}$ for horizontally oriented samples.

4. Vertically oriented samples have a tensile strength three to four times larger than that of horizontally oriented samples. This conclusion confirms the trend noted by Dykins (1970).

Table 2.

Uniaxial Tension Test Data: Saline Samples; -10° C

Sample ID	Ice Type	Fracture or Peak Stress(MPa)*	Strain at Highest Stress ($x10^{-4}$)	Total Strain to Fracture (x10-4)	Initial Tangent Modulus(GPa)
vertical orientation ($\dot{\varepsilon} = 10^{-7}\ s^{-1}$)					
B2VT1	lab	1.06	3.18	3.18	4.1
B3(15)	lab	1.08	5.00	5.00	5.6
B5(14)	lab	1.02	2.59	2.81	5.1
B5(20)	lab	.97	2.59	2.59	5.8
N4T8C1	sea	1.24	2.27	2.27	6.8
N4T2C1	sea	.92	1.36	1.36	5.7
N4T1C1	sea	.92	2.05	2.05	4.0
A3T1C1**	sea	.85	1.64	1.64	7.8
A3T1C12	sea	1.09	2.09	2.09	8.2
horizontal orientation ($\dot{\varepsilon} = 10^{-7}\ s^{-1}$)					
B1HT1	lab	.21	8.3	28.3	1.3
B2HT3	lab	.31	15.0	80.4	2.1
B7(7)	lab	.32	9.1	88.4	2.1
vertical orientation ($\dot{\varepsilon} = 10^{-3}\ s^{-1}$)					
B5(2)	lab	1.03	1.27	1.27	8.1
B5(6)	lab	1.14	.95	.95	8.4
B5(15)	lab	1.12	1.15	1.15	9.0
N4T5C2	sea	.97	.95	.95	8.5
N4T4C2	sea	1.27	1.04	1.04	8.2
A3T3C2	sea	1.57	1.36	1.36	9.1
A3T4C22**	sea	1.54	1.64	1.64	6.7
A3T7C2	sea	1.34	.82	.82	7.6
horizontal orientation ($\dot{\varepsilon} = 10^{-3}\ s^{-1}$)					
B1HT2	lab	.25	.42	.42	4.0
B2HT2	lab	.20	.50	.50	6.0
B7(5)	lab	.44	.54	.54	8.1
B7(8)	lab	.52	.86	.86	5.9

* fracture stresses are reported for all the vertical and the high rate horizontal specimens and peak stresses for the low rate horizontal specimens.

** denotes tests in which only one strain gauge was operational.

Table 3.

Tensile Failure Characteristics; -10° C

	VERTICAL	HORIZONTAL
$\dot{\varepsilon} = 10^{-7} s^{-1}$	fracture in the sample where the column diameter is largest (whether oriented at the top or bottom of test machine); loose flakes on the fracture surface; failure perpendicular to loading direction	shear failure parallel to the growth direction
$\dot{\varepsilon} = 10^{-3} s^{-1}$	cleavage facets on fracture surface; failure perpendicular to loading direction	failure perpendicular to loading direction

Acknowledgements

We wish to thank David Cole, Anthony Gow and Jackie Menge of USA CRREL and Gary Durkee and Roger Howes of the Thayer School Machine Shop for their help and knowledge in the establishment of techniques and equipment. We also thank Dr. Terry D. Ralston of Exxon for supplying the first year sea ice. The work was sponsored by the Office of Naval Research through a University Research Initiative grant (contract no. N00014-86-1C-0695). The experiments were performed in the Ice Research Laboratory of the Thayer School which is supported through funding provided by: Amoco, Exxon, Mobil, Shell, Sohio, Army Research Office, Minerals Management Service, U. S. Coast Guard and the National Science Foundation.

References

Cole, D. M., Gould, L. D., and Burch, W. B., 1985. A system for mounting end caps on ice specimens, *Journal of Glaciology*, Vol. 31, No. 105, p. 362-365.

Cox, G. F. N. and Weeks, W. F., 1983. Equations for Determining the Gas and Brine Volumes in Sea-Ice Samples, *Journal of Glaciology*, Vol. 29, No. 102, p. 306-316.

Dykins, J. E., 1970. Ice Engineering: Tensile properties of sea ice grown in a confined system, Navel Civil Engineering Laboratory Technical Report (R689), 56 pages.

Lee, R. W., 1986. A procedure for testing cored ice under uniaxial tension, *Journal of Glaciology*, Vol. 32, No. 112, p. 540-541.

Lee, R. W. and Schulson, E. M., 1987. The strength and ductility of ice under tension, J. of Offshore Mechanics and Arctic Engineering, in press.

Mellor, M., Cox G. F. N., and Bosworth, H., 1984. Mechanical properties of multi-year sea ice, Testing techniques, CRREL Report 84-8, 39 pages.

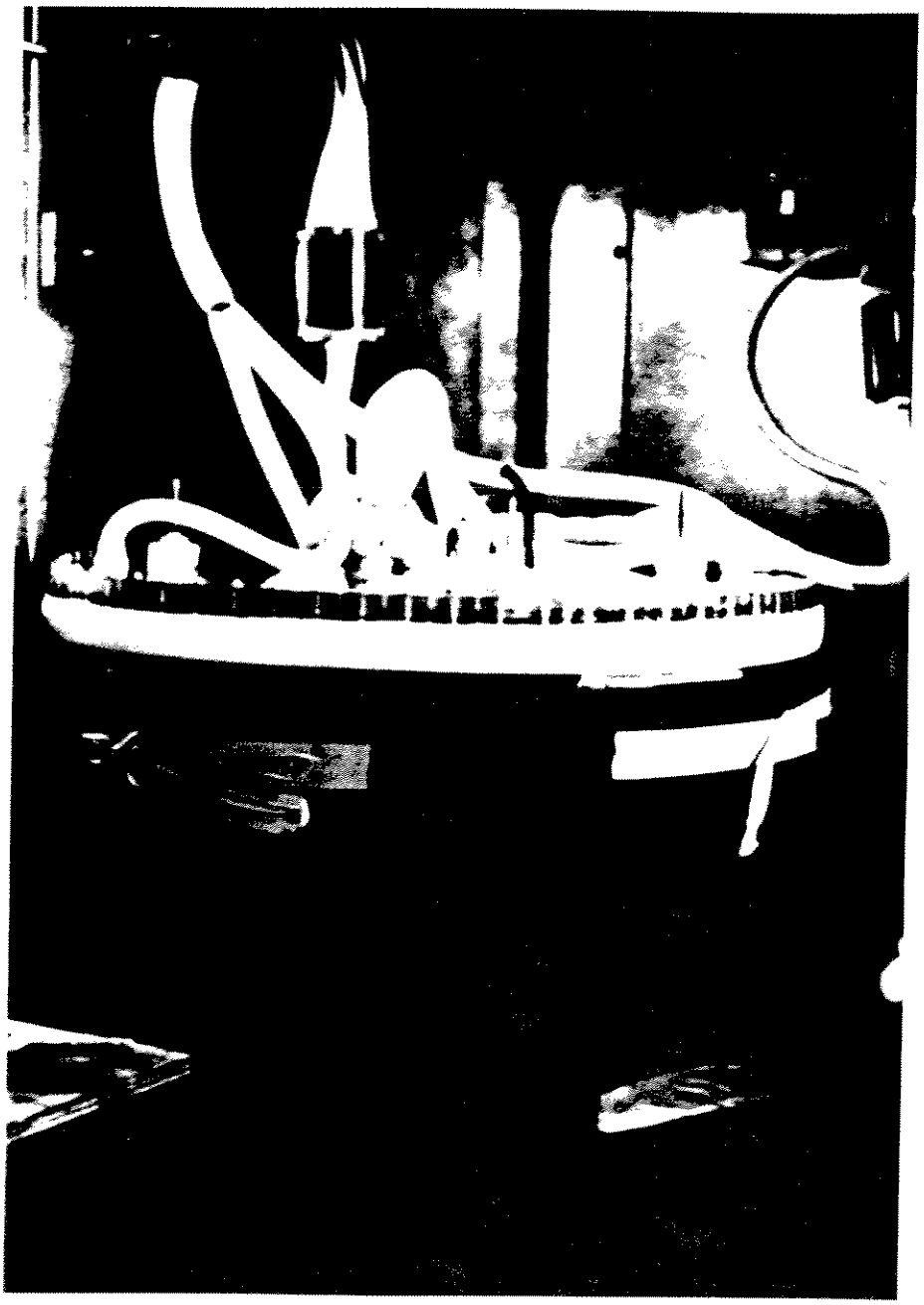

Photograph showing the freezing tank after being insulated. The cooling plate is in position.

Figure 1a.

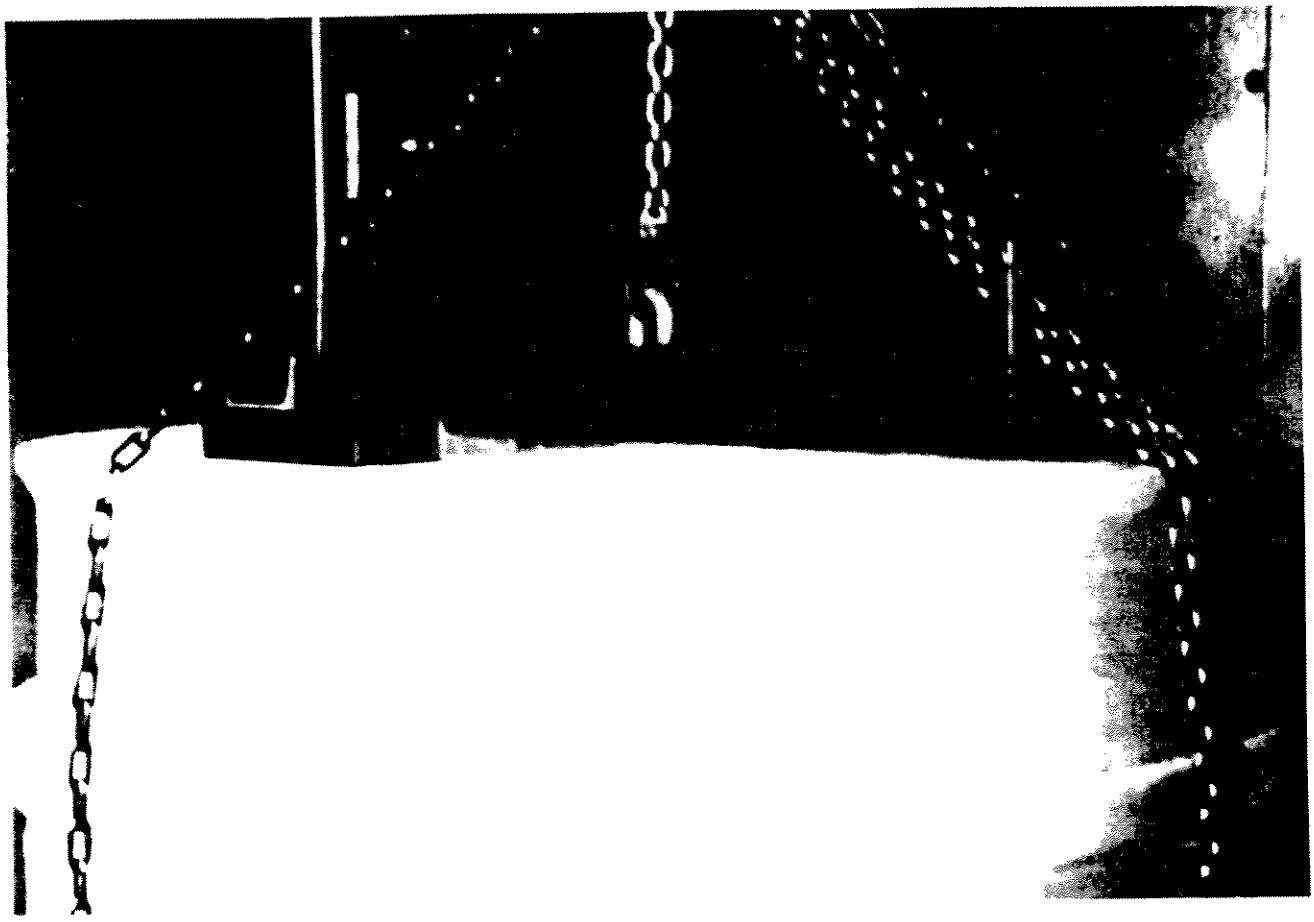

Photograph showing the removal of an ice block of 12-14 inches in thickness.

Figure 1b.

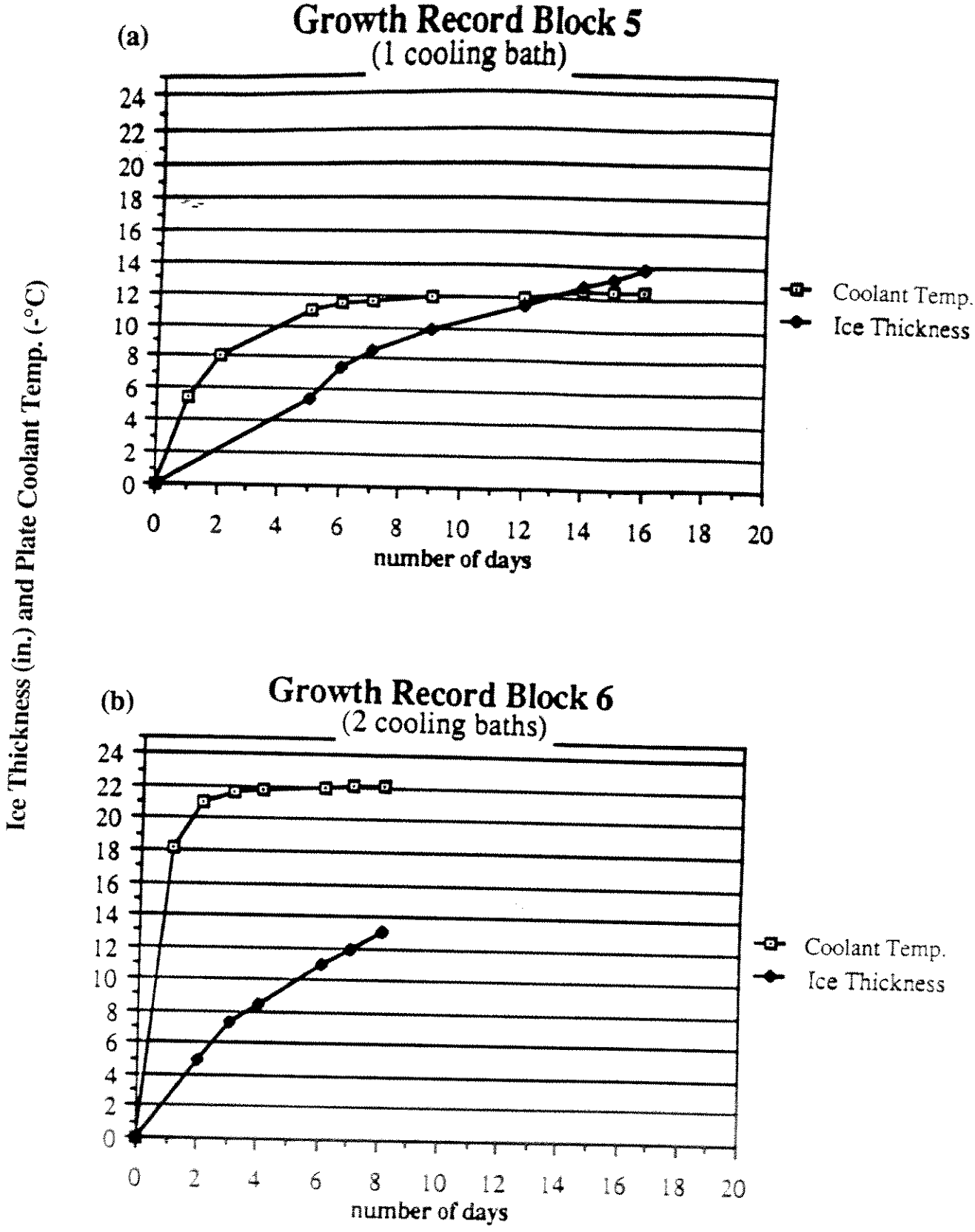

Typical graphs of thickness and coolant temperature versus time for saline ice grown unidirectionally using the apparatus shown in Figures 1a & b.

Figure 2.

A horizontally oriented thin section of Block 3 Core 1 shown by cross polarized illumination. The section was taken in the upper 1/2 - 1 inch of the core.

Figure 3a.

A horizontally oriented thin section taken within the bottom 1 1/2 inches of Block 3 Core 1. Note the larger grains relative to those shown in Figure 3a.

Figure 3b.

A vertically oriented thin section from the upper half of Block 3, Core 1.

Figure 3c.

A horizontally oriented thin section of first year sea ice gathered in November of 1984 from the Alaskan Beaufort Sea.

Figure 4.

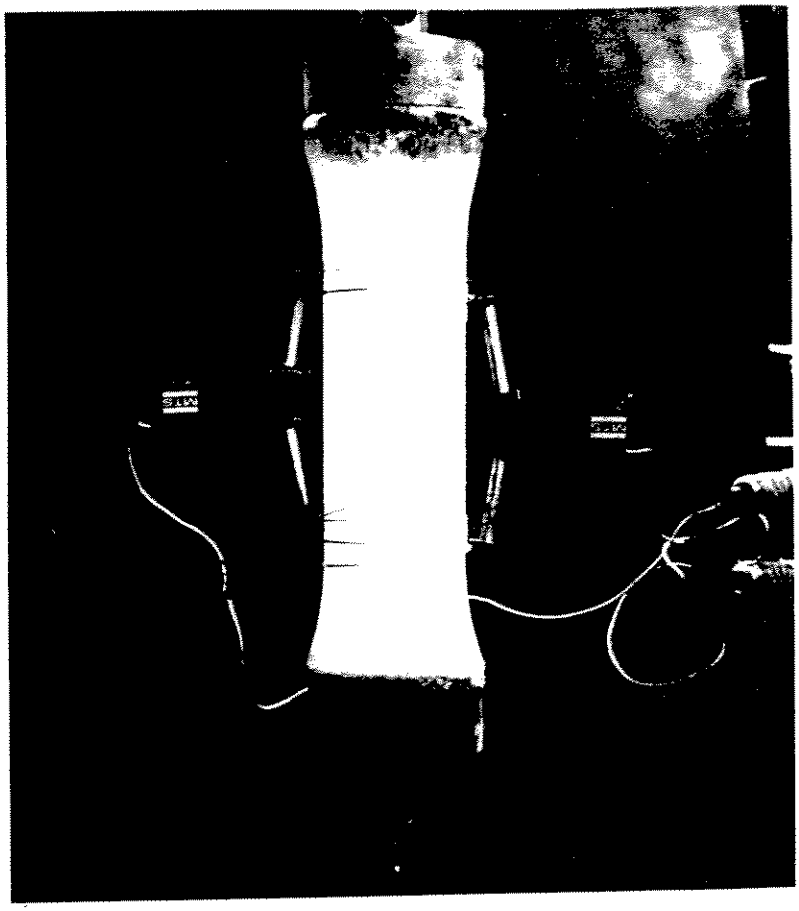

A photograph showing an instrumented test specimen used in the high strain rate ($10^{-3}s^{-1}$) tension test. The specimen is necked so that stresses over 1 MPa are obtainable without end-cap failures. The extensometers are attached by rubber bands and seat on felt pads frozen to the sample. Specimen B5(5).

Figure 5.

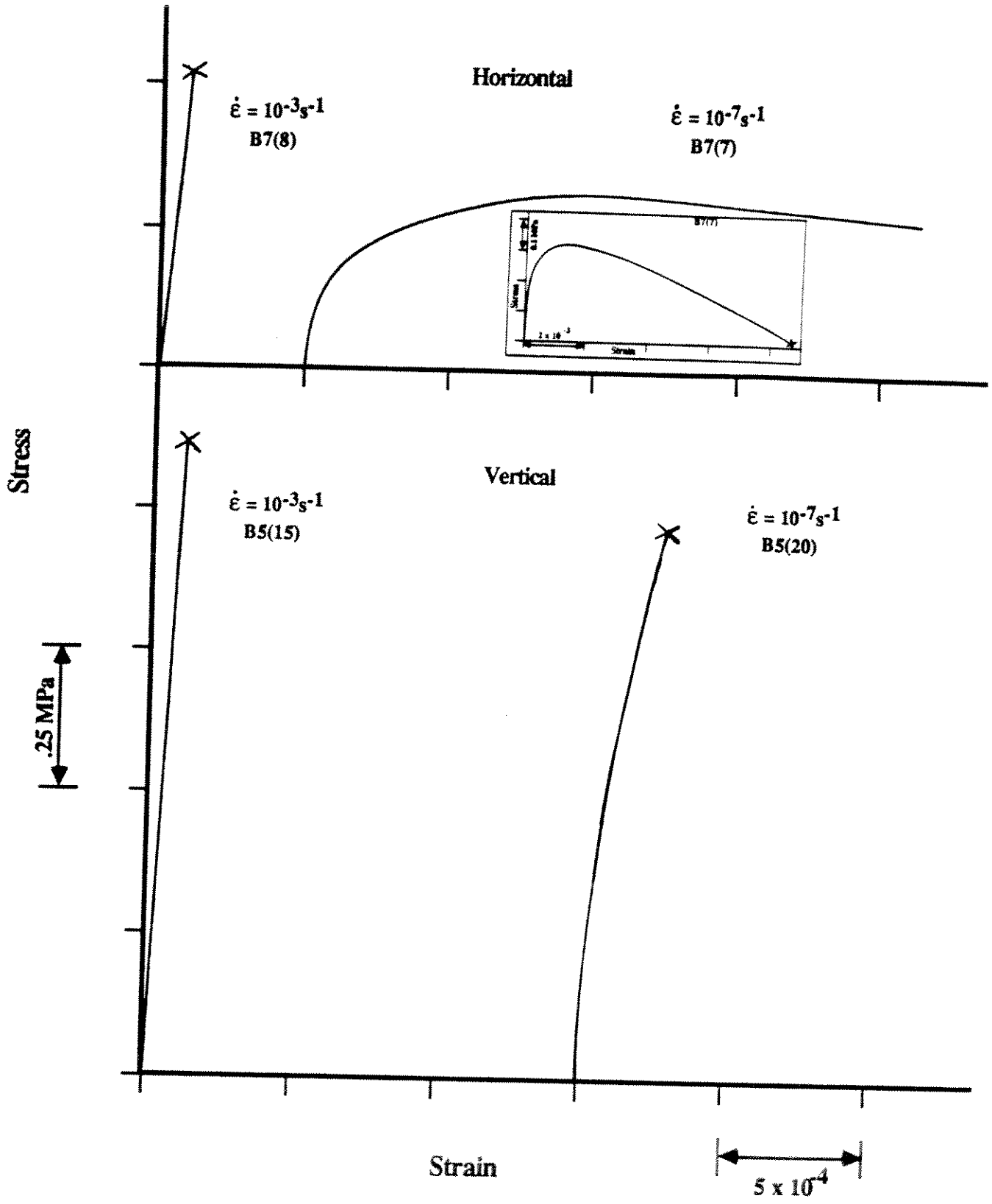

Typical stress-strain curves of columnar saline ice tested at -10° C under uniaxial tension. The X denotes fracture. The inset shows the complete curve of specimen B7(7).

Figure 6.

Stress vs. Stain Rate; Tension Tests: -10C

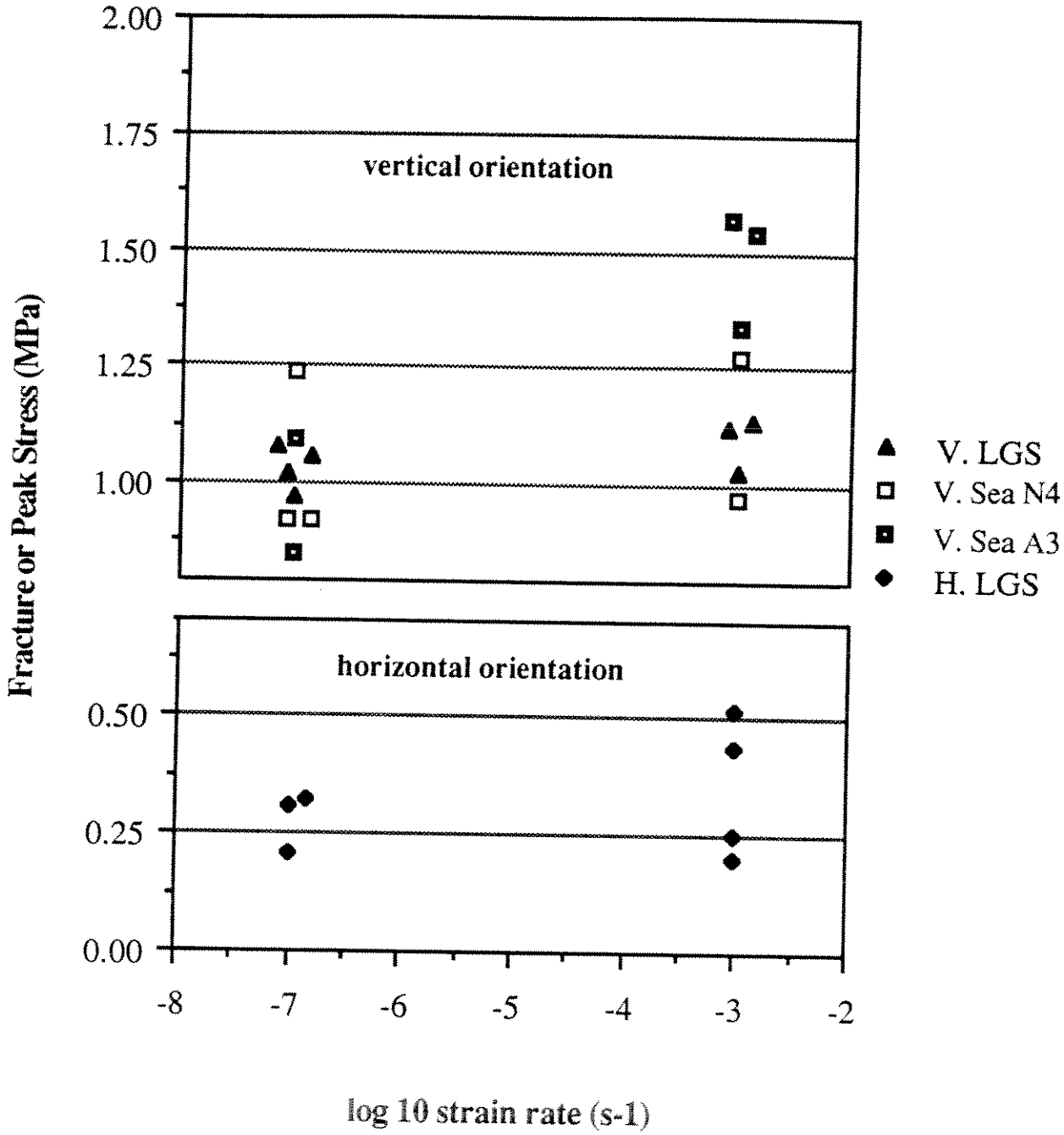

Saline uniaxial tension test data. Tests were performed at -10° C.
N4 and A3 mean respectively, ice harvested in November, 1984 and April, 1983.

Figure 7.

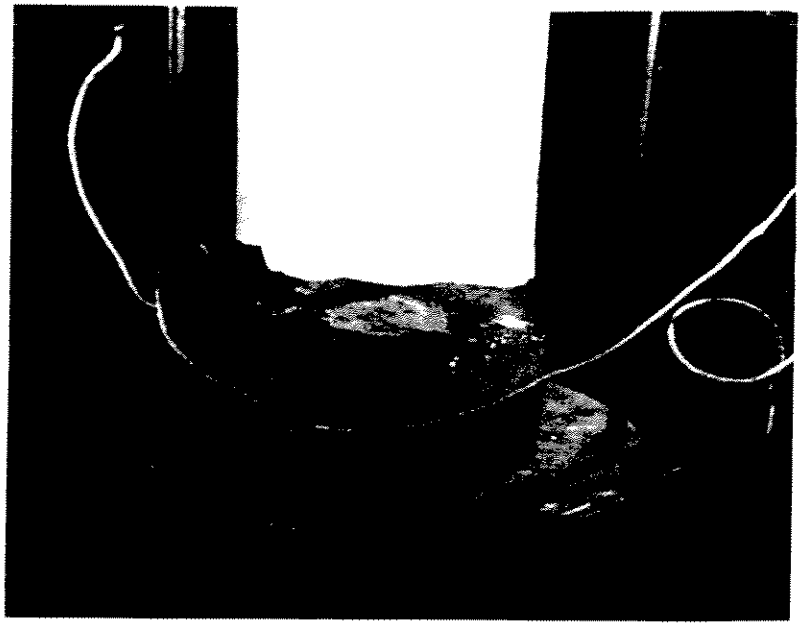

The $\dot{\varepsilon} = 10^{-7}s^{-1}$ vertically oriented samples break where the columns are largest in diameter, regardless to the samples orientation in the testing machine. Here, the specimen is shown as having broken near its lower end which corresponds to the bottom of the parent block. Often there are loose flakes on the fracture surface. Specimen B5(14).

Figure 8.

The $\dot{\varepsilon} = 10^{-3}s^{-1}$ vertically oriented cores break in the top two-thirds of the necked region and there are cleavage facets on the fracture surface. The star denotes the origin of the crack which propagated to cause fracture.

Figure 9.

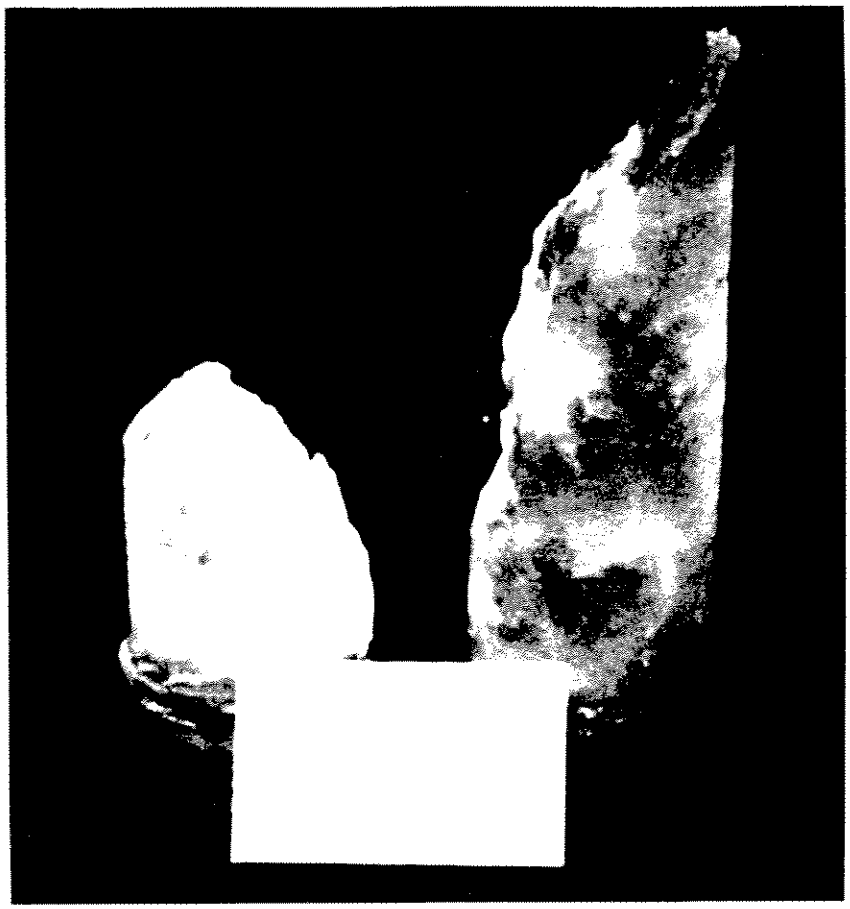

The horizontally oriented $\dot{\varepsilon} = 10^{-7}s^{-1}$ samples fail by means of a shear failure parallel to the growth direction.

Figure 10.

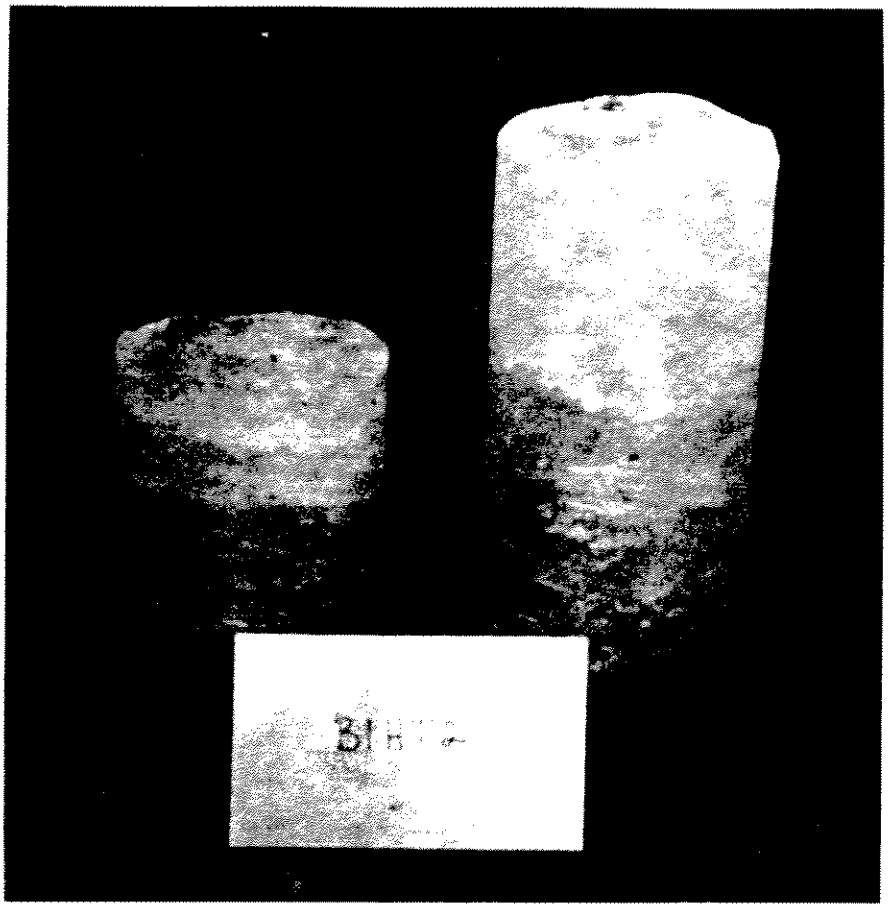

The $\dot{\varepsilon} = 10^{-3}s^{-1}$ horizontally oriented cores fail perpendicular to the loading direction.

Figure 11.